

New Determination of the Astrophysical S Factor S_{E1} of the $^{12}\text{C}(\alpha, \gamma)^{16}\text{O}$ Reaction

X. D. Tang,^{1,*} K. E. Rehm,¹ I. Ahmad,¹ C. R. Brune,² A. Champagne,³ J. P. Greene,¹ A. A. Hecht,^{1,4} D. Henderson,¹ R. V. F. Janssens,¹ C. L. Jiang,¹ L. Jisonna,⁵ D. Kahl,^{1,†} E. F. Moore,¹ M. Notani,^{1,6} R. C. Pardo,¹ N. Patel,^{1,7} M. Paul,⁸ G. Savard,¹ J. P. Schiffer,¹ R. E. Segel,⁵ S. Sinha,^{1,‡} B. Shumard,¹ and A. H. Wuosmaa⁹

¹Physics Division, Argonne National Laboratory, Argonne, Illinois 60439, USA

²Ohio University, Athens, Ohio 45701, USA

³University of North Carolina, Chapel Hill, North Carolina 27599, USA

⁴University of Maryland, College Park, Maryland 20742, USA

⁵Northwestern University, Evanston, Illinois 60208, USA

⁶Michigan State University, East Lansing, Michigan 48824, USA

⁷Colorado School of Mines, Golden, Colorado 80401, USA

⁸Hebrew University, Jerusalem, Israel

⁹Western Michigan University, Kalamazoo, Michigan 49008, USA

(Received 16 March 2007; published 3 August 2007)

A new measurement of the β -delayed α decay of ^{16}N has been performed using a set of high efficiency ionization chambers. Sources were made by implantation of a ^{16}N beam, yielding very clean α spectra down to energies as low as 400 keV. Our data are in good agreement with earlier results. For the S factor S_{E1} , we obtain a value of 74 ± 21 keV b. In spite of improvements in the measurement, the error in S_{E1} remains relatively large because of the correlations among the fit parameters and the uncertainties inherent to the extrapolation.

DOI: 10.1103/PhysRevLett.99.052502

PACS numbers: 21.10.Pc, 23.60.+e, 25.55.-e, 26.20.+f

The main isotopes of carbon and oxygen (^{12}C and ^{16}O), crucial to all living organisms, are produced by helium burning in red giant stars. The ratio of their abundances is determined by the competition between the triple- α process ($\alpha + \alpha + \alpha \rightarrow ^{12}\text{C}$) and the $^{12}\text{C}(\alpha, \gamma)^{16}\text{O}$ reaction. This ratio also affects the future evolution of a star during its carbon, neon, and oxygen burning phases [1]. While the cross section for the triple- α process is experimentally quite well determined [2], our knowledge of the $^{12}\text{C}(\alpha, \gamma)^{16}\text{O}$ reaction under red giant conditions ($E_\alpha \sim 300$ keV) is considered to be the most serious uncertainty in nucleosynthesis [1,3]. There are two main α -capture modes for the $^{12}\text{C}(\alpha, \gamma)^{16}\text{O}$ reaction. One is capture with multipolarity $E1$ with contributions from the 1^- resonance at $E_{\text{cm}} = 2.418$ MeV ($E_x = 9.585$ MeV) and the subthreshold 1^- state at $E_{\text{cm}} = -45$ keV ($E_x = 7.117$ MeV), a channel that is isospin forbidden. The $E2$ capture mode includes contributions from direct capture and the tail from a 2^+ ($E_{\text{cm}} = -245$ keV, $E_x = 6.917$ MeV) subthreshold state. Contributions from cascade transitions are expected to be small [4]. At $E_{\text{cm}} \sim 300$ keV, the cross sections are of the order of 10^{-17} b, i.e., beyond present experimental capabilities. One has, therefore, to rely on extrapolations [5] using measurements above ~ 890 keV [6–11]. The values quoted in the recent NACRE compilation [12] are 79 ± 21 keV b (S_{E1}) and 120 ± 60 keV b (S_{E2}), respectively. In this Letter, $S_{E1,E2}$ refer to the S factors at $E_{\text{cm}} = 300$ keV.

Measurements of the β -delayed α decay of ^{16}N provide the tightest constraints for determining S_{E1} [5]. In these experiments, S_{E1} is extracted from the height of a small satellite peak located at $E_{\text{cm}} \sim 1$ MeV in the α -energy

spectrum. This peak originates from the interference between the subthreshold 1^- state ($E_x = 7.117$ MeV) and the higher-lying 1^- state in ^{16}O at $E_x = 9.585$ MeV [13]. The very small branching ratio of the ^{16}N decay ($\sim 10^{-5}$) complicates the α -decay experiments in two ways: It requires a strong and pure source of ^{16}N particles, and the high β background severely masks the low-energy part of the α spectrum in the vicinity of the small satellite peak from which S_{E1} is obtained. This peak has been studied by several groups [5,14,15], all of them using thin Si-surface barrier detectors, which are sensitive to β particles, have dead layers, and are prone to deterioration during measurements lasting several weeks.

Because of the importance of the $^{12}\text{C}(\alpha, \gamma)^{16}\text{O}$ reaction, we have remeasured the ^{16}N decay using a different approach. To reduce the sensitivity to electrons, we developed an array of high-acceptance ionization chambers of minimal thickness, to be used for the coincident detection of ^{12}C and α particles following the ^{16}N decay. The main goals of the experiment, described below, were (1) to remeasure the height of the small satellite α peak, using a different experimental setup, subject to different systematic uncertainties, (2) to extend the measurements towards lower energies and, (3) to resolve the discrepancies, observed in earlier measurements, in the shape of the low-energy part of the α spectrum [5,14–16].

A schematic of the experimental setup is given in Fig. 1. A 61-MeV ^{16}N ($T_{1/2} = 7.1$ sec) beam is slowed down in a gas-filled cell and stopped in a thin carbon foil (foil a) mounted on a rotating wheel (diameter 18.7 cm) located in the main part of the detection chamber. The cell and the main chamber are filled with P10 counting gas at a pressure

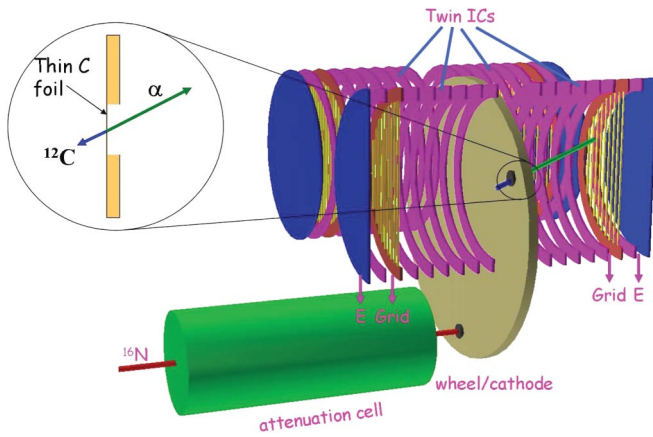


FIG. 1 (color). Schematic of the experimental setup used for a measurement of the β -delayed α decay of ^{16}N .

of 150 Torr. After an irradiation of 15 s, the foil (a) is rotated (in 60 ms) by 120° , placing it between a pair of twin-ionization chambers (pair I) for the coincident detection of ^{12}C - α pairs. The carbon foil is counted in this pair of ionization chambers (IC) for 15 sec. During this time, a second foil (b), positioned on the wheel 120° relative to the first foil, is irradiated. At the end of the second irradiation, foil (b) is rotated to be between a second pair of ionization chambers (pair II) and counted, while foil (a) is again irradiated with ^{16}N . Detector pair I is meanwhile counting a nonirradiated foil to establish backgrounds. The same foil, which is never irradiated, is also used for measuring the background in detector pair II. In order to check the background in the gas system of the ionization chambers, some of the measurements were performed with a 15-s-on, 15-s-off cycle.

The ionization chambers are of the twin-ionization type, frequently used for the coincident detection of fission fragments [17,18]. In addition to the energy signal from the anode, an angle signal is obtained from the Frisch grid [18]. Details of the technique will be given in a forthcoming paper. The ionization chambers were calibrated with α sources (^{228}Th and ^{148}Gd) as well as with α - ^7Li and α -triton coincidences obtained from the $^{10}\text{B}(n, \alpha)^7\text{Li}$ and $^6\text{Li}(n, \alpha)t$ reactions, respectively, using moderated neutrons from a Pu-Be neutron source. The latter two reactions provided α particles of 1.472, 1.776, and 2.056 MeV, energies that bracket the energy range of interest. The linearity of the electronics was tested with a precision pulser. The energy resolution obtained from the 1.472-MeV line is 40 keV. The accuracy of the calibration is better than ± 5 keV. The long-term stability of the detectors was monitored daily over a period of 10 days with α 's from the $^{10}\text{B}(n, \alpha)^7\text{Li}$ reaction and was found to be better than 3×10^{-3} .

To test the sensitivity of the ionization chambers to β particles, a ^{22}Na β^+ source with an activity of about 10^5 decays/s was mounted on the target wheel. The strength of this source is similar to the actual rate of β

particles from ^{16}N in the experiment. The only change observed in the spectrum was a 25% increase in the singles count rate at very low energies ($E \sim 100$ keV), corresponding to an increase in count rate to about 170 counts/hr above the threshold of 100 keV. For the coincidence measurement, this background rate is negligible.

In the present experiment, the ^{16}N beam was produced via the In-Flight Technique [19], by bombarding a deuterium-filled cryogenic gas cell with an 82-MeV beam of ^{15}N from the ATLAS facility. No $^{17,18}\text{N}$ ions can be produced in this process. All beam contaminants are stable and, therefore, do not bring radioactivities to the target. With $6 \times 10^{11}/\text{s}$ ^{15}N incident on the deuterium-filled production cell, the ^{16}N beam intensity measured behind the catcher foil was about $3 \times 10^6/\text{s}$.

The thickness of the carbon foils used to stop the ^{16}N ions after the absorption cell (nominally $10 \mu\text{g}/\text{cm}^2$) was measured after the experiments through the energy loss of ^{228}Th α particles using a Split Pole spectrograph and was found to be $17 \pm 2 \mu\text{g}/\text{cm}^2$. The fraction of ^{16}N stopped in the foil was measured to be about 5%, in good agreement with estimates.

In a study of the ^{16}N β -delayed α decay, three aspects are important: (1) α particles with energies down to 0.6 MeV have to be detected in coincidence with ^{12}C ions of even lower energies (~ 0.1 MeV). Any significant energy loss of the outgoing particles in the catcher foil will deform the shape of the spectrum. (2) If a particle, emitted from the foil, is stopped in the support frame, only a part of the energy is deposited in the gas. Such events must be clearly separated from the true coincidence events producing the interference peak. (3) The detection efficiency must be constant over the energy range from 0.2 MeV to 2 MeV. Calibration measurements with pulser signals showed that the coincidence efficiency was constant down to 120 keV. The geometry of the target wheel and the detectors was optimized by Monte Carlo simulations. For a beam spot of ~ 5 mm, the foil was mounted on one side of a 1.75 mm thick target frame with a hole of 10 mm (see insert in Fig. 1). Because of the upstream-downstream asymmetry of the target frame, the α - ^{12}C coincidences exhibit slight differences depending on the direction in which the α particle is emitted, as can be seen in Fig. 2, where coincident events measured in the upstream and downstream detectors are shown. On the left, the results for a foil implanted with ^{16}N particles are given, while the right panel represents the background measurement mentioned above. The two groups with the highest count rate seen in Fig. 2(a) correspond to ^{12}C - α coincidences in the upstream and downstream detectors, respectively. These two groups exhibit a tail caused by energy-loss straggling of the ^{12}C particles in the capture foil. The group observed very close to the y-axis (around channel 2000) is caused by ^{16}N decays where the ^{12}C particle (emitted downstream) is stopped in the target frame, so that only part of the corresponding energy is detected (see the insert in Fig. 1). Such

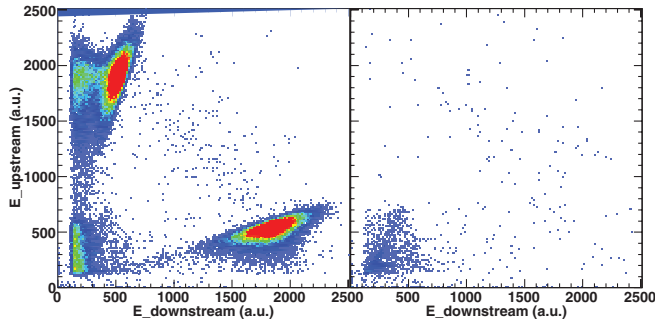


FIG. 2 (color). (Left) coincident energy spectrum, measured with one of the twin-ionization detectors for a foil with implanted ^{16}N particles. (Right) same as above, but for a non-implanted foil.

events can be eliminated by using the angle information from the twin-ionization chambers. An α particle, emitted downstream and hitting the target frame with only a fraction of the α energy detected in the ionization chamber, gives rise to the group seen near the origin.

Here, we only discuss events where the α particle is emitted downstream and the full ^{12}C energy is recorded, represented by the events in the lower part of Fig. 2(a). A discussion of all events will be given in the future.

Selecting events below channel 800, and requiring the correct pulse height ratio of $\alpha/^{12}\text{C}$ events (as done in [5]), results in the α spectrum given in Fig. 3(a). The additional requirement that all particles are in the correct Frisch-grid

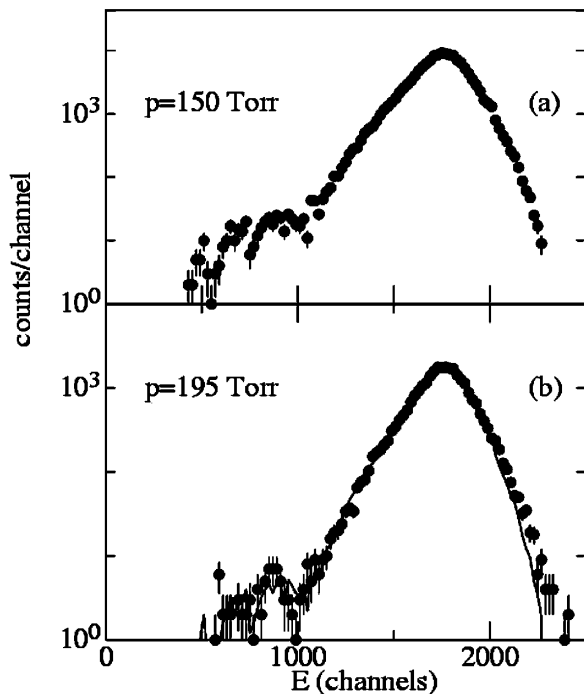


FIG. 3. (a) The α spectrum measured in one of the twin-ionization chambers filled with 150 Torr of isobutane. (b) Same as (a), but at a pressure of 195 Torr. The solid line is the spectrum obtained at 150 Torr, scaled in height.

anode region (see [18] for details) of the upstream (^{12}C) and downstream (α) ionization chambers changes the number of counts in the region of the satellite peak by less than 1%. While the pressure of 150 Torr (equivalent to a Si detector thickness of $7\ \mu\text{m}$) minimizes the interference from the low-energy α particles stopped in the target frame (giving rise to the group next to the origin in Fig. 2), it also leads to a distortion of the α spectrum at channel numbers above ~ 2000 (corresponding to energies above 1.9 MeV) due to incomplete stopping of higher energy α particles. To verify this, some of the measurements were performed at a pressure of 195 Torr [Fig. 3(b)]. At this pressure, particles up to 2.4 MeV are stopped in the ionization chamber. The solid line in Fig. 3(b) represents the normalized spectrum obtained at 150 Torr and illustrates the effects of incomplete stopping. These effects were also reproduced in Monte Carlo simulations. Correcting the 150 Torr data at energies above an α energy of 1.9 MeV, we obtain a summed spectrum shown in Fig. 4 containing 2.2×10^5 events. This number will be doubled in the final analysis. Due to the insensitivity of ionization chambers to the copious β 's, the low-energy satellite peak in the β -delayed α spectrum of ^{16}N can now be followed, practically background-free and without correcting for pileup events from electrons or contributions from $^{17,18}\text{N}$ decays, down to a c.m.-energy of ~ 600 keV. The solid line is the result of an R -matrix fit, which is discussed below.

The insert in Fig. 4 shows a comparison of our α spectrum with the results from earlier experiments. The lines correspond to the spectra from [5] (dashed line) and [14] (solid line), normalized in height to the present experiment. While these previous experiments agree on the high-energy side of the spectrum, they show disagreements for the low-energy part of the main peak, with [14] exhibiting a shallower slope, when compared to [5]. In this energy region, our spectrum is in better agreement with the data of [14]. The height of the interference peak at

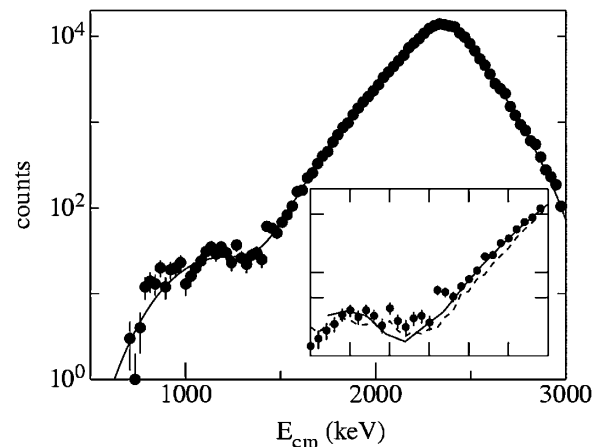


FIG. 4. Summed α spectrum obtained in this experiment in comparison with an R -matrix fit. The insert shows the low-energy part of spectrum together with the previous results (solid [14] and dashed lines [5]). See text for details.

TABLE I. S_{E1} values obtained from R -matrix fits with different input parameters. See text for details.

source of ^{16}N data	S_{E1} keV b	χ^2	other data used in fits
Ref. 5	79 ± 21	1.6	
this work	74 ± 21	2	standard input
	88 ± 18	2.9	phase shifts from [21]
	70 ± 20	2	new β -branching ratio [23]
	73 ± 21	1.7	with (α, γ) data from [8]
	77 ± 23	2	constant + linear term
	85 ± 18	2.7	Ref. [8,21,23]

$E_{\text{cm}} \sim 1$ MeV, which is sensitive to the S factor, shows good agreement among the different experiments.

Extracting the relevant S factor S_{E1} from the data is usually done using the R -matrix formalism through a least-squares fit to data from the β -delayed α decay of ^{16}N , in combination with experimental results from the capture reaction $^{12}\text{C}(\alpha, \gamma)^{16}\text{O}$ performed at higher energies, as well as with phase shift parameters obtained from elastic scattering of $^{12}\text{C}(\alpha, \alpha)$. For this, we have used the R -matrix program from [20]. The number of fitting parameters is large (typically 14), and there are strong correlations among some of the parameters, even for high-statistics data. In a first step, we have employed the same phase shift and direct capture data as used in [5,14] for the R -matrix calculations. The result of such a fit (with a channel radius $a = 6.5$ fm) is given by the solid line in Fig. 4. We obtain $S_{E1} = 74 \pm 21$ keV b, including a systematic uncertainty of 10 keV b, which is dominated by the ± 5 keV uncertainty of the energy calibration.

There are new data available for some of the other inputs used in the fits. With the phase shift data of [2,21], which are not yet available in tabulated form, the S_{E1} value obtained from our fits increases to 88 ± 18 keV b, which is closer to the value ($S_{E1} = 101 \pm 17$ keV b) obtained in [22]. A similar sensitivity of S_{E1} to the input parameters of the R -matrix calculation was observed when the β -branching ratio of the subthreshold 1^- state was increased by $\sim 10\%$, as suggested by a recent experiment [23]. Using the new set of capture data from [8–10], however, does not change S_{E1} appreciably. In the previous R -matrix fits, a distant 1^- resonance was introduced, which in [5] was found to be at $E_x \sim 19$ MeV. No independent evidence for this resonance exists. Varying the location of this “background state” between 15 and 25 MeV changes S_{E1} by ± 10 keV b. We have also carried out fits that include a constant plus linearly energy-dependent term, instead of the additional resonance, which gives $S_{E1} = 77 \pm 23$ keV b. The S_{E1} factor obtained by using all available (but partially unpublished) data in the fit is 85 ± 18 keV b. These strong sensitivities to the input parameters indicate that improved measurements for all input parameters as well as a better theoretical description are needed in order to reduce the uncertainties in the $^{12}\text{C}(\alpha, \gamma)^{16}\text{O}$ rate.

We have performed a new measurement of the β -delayed α decay of ^{16}N using a setup that is insensitive to the high electron background. The low-energy part of the spectrum was found to be in better agreement with earlier data measured at Mainz [16] and Yale [14] than with the data from the TRIUMF [5] group. The satellite peak, which originates from the interference between the sub-threshold 1^- state and the higher-lying 1^- level in ^{16}O , was clearly resolved. Its height is in agreement with earlier measurements. The extrapolation of S_{E1} to regions where it cannot be measured directly involves input from many parameters, such as phase shifts, capture cross sections, branching ratios and contributions from nonresonant amplitudes. Our analysis shows that improvements in the accuracies of all these values are needed in order to reduce the uncertainty of S_{E1} .

We would like to thank the operations group of the ATLAS accelerator for providing the ^{16}N beam for the experiment. This work was supported by the US Department of Energy, Office of Nuclear Physics, under Contract No. DE-AC02-06CH11357 and by the NSF Grant No. PHY-02-16783 (Joint Institute for Nuclear Astrophysics).

*Currently at University of Notre Dame, Notre Dame, IN, USA

†Currently at McMaster University, Hamilton, Canada

‡Currently at University of CA, Davis, CA, USA

- [1] T. A. Weaver and S. Woosley, Phys. Rep. **227**, 65 (1993).
- [2] L. R. Buchmann and C. A. Barnes, Nucl. Phys. **777**, 254 (2006).
- [3] W. Fowler, Rev. Mod. Phys. **56**, 149 (1984).
- [4] C. Matei *et al.*, Phys. Rev. Lett. **97**, 242503 (2006).
- [5] R. Azuma *et al.*, Phys. Rev. C **50**, 1194 (1994); L. Buchmann *et al.*, Phys. Rev. Lett. **70**, 726 (1993).
- [6] A. Redder *et al.*, Nucl. Phys. A **462**, 385 (1987).
- [7] J. M. L. Ouellet *et al.*, Phys. Rev. Lett. **69**, 1896 (1992).
- [8] R. Kunz *et al.*, Phys. Rev. Lett. **86**, 3244 (2001).
- [9] R. Kunz *et al.*, Astrophys. J. **567**, 643 (2002).
- [10] M. Assunção *et al.*, Phys. Rev. C **73**, 055801 (2006).
- [11] R. Plag, Ph.D. thesis, FZ Karlsruhe [FZKA Report No. 7099, 2005].
- [12] C. Angulo *et al.*, Nucl. Phys. A **656**, 3 (1999).
- [13] J. Humblet, Phys. Rev. C **42**, 1582 (1990).
- [14] Z. Zhao *et al.*, Phys. Rev. Lett. **70**, 2066 (1993).
- [15] R. H. France *et al.*, Nucl. Phys. A **621**, 165c (1997).
- [16] K. Neubeck, H. Schober, and H. Wäffler, Phys. Rev. C **10**, 320 (1974).
- [17] C. Budtz-Jørgensen *et al.*, Nucl. Instrum. Methods Phys. Res., Sect. A **258**, 209 (1987).
- [18] A. Göpfert, F.-J. Hamsch, and H. Bax, Nucl. Instrum. Methods Phys. Res., Sect. A **441**, 438 (2000).
- [19] B. Harss *et al.*, Rev. Sci. Instrum. **71**, 380 (2000).
- [20] J. Powell, Ph.D. thesis, University of Toronto, 1994.
- [21] P. Tischhauser *et al.*, Phys. Rev. Lett. **88**, 072501 (2002).
- [22] C. Brune *et al.*, Phys. Rev. Lett. **83**, 4025 (1999).
- [23] K. E. Rehm *et al.* (to be published).